SAND2020-2409C
Proceedings of the ASME 2020
Power Conference
POWER2020
August 2 – 6, 2020, Anaheim, CA, USA

POWER2020-####

THE SANDIA NATIONAL LABORATORIES[1] NATURAL CIRCULATION COOLER

Bobby D. Middleton[1#], Patrick V. Brady[1], Serafina Lawles

[1]Sandia National Laboratories, Albuquerque, NM
[#]Corresponding Author

ABSTRACT

Sandia National Laboratories (SNL) is developing a cooling technology concept – the Sandia National Laboratories Natural Circulation Cooler (SNLNCC) – that has potential to greatly improve the economic viability of hybrid cooling for power plants. The SNLNCC is a patented technology that holds promise for improved dry heat rejection capabilities when compared to currently available technologies. The cooler itself is a dry heat rejection device, but is conceptualized here as a heat exchanger used in conjunction with a wet cooling tower, creating a hybrid cooling system for a thermoelectric power plant.

The SNLNCC seeks to improve on currently available technologies by replacing the two-phase refrigerant currently used with either a supercritical fluid – such as supercritical CO_2 (sCO_2) – or a zeotropic mixture of refrigerants. In both cases, the heat being rejected by the water to the SNLNCC would be transferred over a range of temperatures, instead of at a single temperature as it is in a thermosyphon. This has the potential to improve the economics of dry heat rejection performance in three ways: decreasing the minimum temperature to which the water can be cooled, increasing the temperature to which air can be heated, and increasing the fraction of the year during which dry cooling is economically viable. This paper describes the experimental basis and the current state of the SNLNCC.

Keywords: Sandia National Labs, Natural Circulation Cooler, Dry Cooling, Dry Heat Rejection, Hybrid Cooling, Supercritical CO_2, Zeotropic Fluids.

NOMENCLATURE

A_c	Cross-sectional area
c_p	Specific heat capacity
D	Diameter
F	Ratio of air needed to reject maximum heat possible with SNLNCC
g	Gravitational acceleration
Gr	Grashof number
H	Loop height
L_t	Total loop length
$\dot{m}$	Mass flow rate
Q	Heat rate
T_w	Wall temperature
T_B	Bulk temperature
U	Mean fluid velocity
β	Volumetric coefficient of expansion
ρ	Density
μ	Dynamic viscosity
υ	Kinematic viscosity

SUBSCRIPTS AND SUPERSCRIPTS

2p	Two-phase
Air	Air
H2O	Water
SC	Supercritical
ss	Steady state

1. INTRODUCTION

Thermoelectric power production using wet cooling is responsible for more than 45% of all water withdrawals in the United States (US) [1]. Lack of water for wet cooling increasingly limits power generation [2, 3].

Wet cooling involves either once-through cooling or recirculating evaporative cooling. Once-through cooling withdraws water (typically from a nearby large body of water), heats it in a steam condenser with waste heat from the power plant, then returns it to the source at a higher temperature, but still as a subcooled liquid. The water is withdrawn; but not consumed. A recirculating cooling system withdraws water, heats it in a steam condenser, then passes it through a cooling tower so that a portion of it evaporates (thereby removing the waste heat), and recirculates the remaining water back to the condenser. The evaporated water is consumed. Once-through systems typically *withdraw* 40-100 times as much water as evaporative cooling systems [4]. Recent Environmental Protection Agency (EPA) regulations encourage utilities to

[1] *This paper describes objective technical results and analysis. Any subjective views or opinions that might be expressed in the paper do not necessarily represent the views of the U.S. Department of Energy or the United States Government.*

Sandia National Laboratories is a multimission laboratory managed and operated by National Technology & Engineering Solutions of Sandia, LLC, a wholly owned subsidiary of Honeywell International Inc., for the U.S. Department of Energy's National Nuclear Security Administration under contract DE-NA0003525.

utilize evaporative cooling instead of once-through cooling [5], which should lead to a *lower rate of water withdrawal*, but a *higher rate of water consumption*.

Only 3% of thermoelectric generation uses low water dry or hybrid cooling [6]. Hybrid cooling systems provide dry cooling during the coolest times of the year and wet cooling during the rest of the year. Dry cooling is either direct or indirect. In direct dry cooling systems, turbine exhaust steam is condensed in an air-cooled condenser. With indirect dry cooling, steam is condensed in a water-cooled condenser. The coolant is then cooled in a water-to-air heat exchanger. For existing plants using wet cooling, a transition to direct dry cooling is unlikely for a couple reasons. First, the air-cooled condensers (ACCs) would need to be in close proximity to the steam turbines. Due to the large size of typical ACCs, there simply may not be adequate space available at existing power plants. Secondly, since the condensation in ACCs is in direct contact with finned heat exchanger surfaces, ACCs are subject to freezing and sometimes explosions. This puts the main steam loop in jeopardy of being breached and the coolant expelled. This would be economically catastrophic, and in the case of nuclear power, could also place the reactor at risk.

Existing plants – especially nuclear plants – are more likely to try to use some form of indirect dry cooling technology. But since dry cooling becomes less attractive at high ambient temperatures due to plant efficiency penalty, indirect dry cooling technology would likely be coupled with existing cooling towers to form a hybrid cooling system.

In 2014, Sandia National Laboratories (Sandia) demonstrated the high natural circulation potential of supercritical carbon dioxide (sCO_2), a key requirement for effective working fluids in decay heat rejection. Natural circulation occurs in an engineered system when a fluid flows without use of a pump or compressor. The fluid in an enclosed loop is heated at one point and cooled at another point to create a density difference; the density difference then drives circulation through the loop. The driving force is proportional to the difference in densities and the height difference between the cold and hot portions of the fluid (Figure 1 [9, 11]).

The most important characteristic of a natural circulation candidate fluid is a large change in density with temperature, measured by, for example, the Grashof number. The Grashof number is a dimensionless number that approximates the ratio of buoyancy to viscous forces in a fluid. For a pipe, the Grashof number is:

$$Gr = \frac{g\beta(T_W - T_B)D^3}{\upsilon^2}. \quad (1)$$

Table 1 compares the Grashof numbers of CO_2 and water (divided by the cube of the characteristic length) for a bulk fluid temperature of 300 K and a wall temperature of 310 K at a pressure of 7.69 MPa. These conditions place the fluid very near the critical point for CO_2, which has a critical temperature of 304.1 K and a critical pressure of 7.38 MPa [9, 11]. Although the Grashof number is not the only factor to consider when evaluating a fluid for potential use in a naturally circulating decay heat removal system, the fact that the Grashof number for is four orders of magnitude greater than that of water in this regime indicates that CO_2 is an excellent candidate for further investigation.

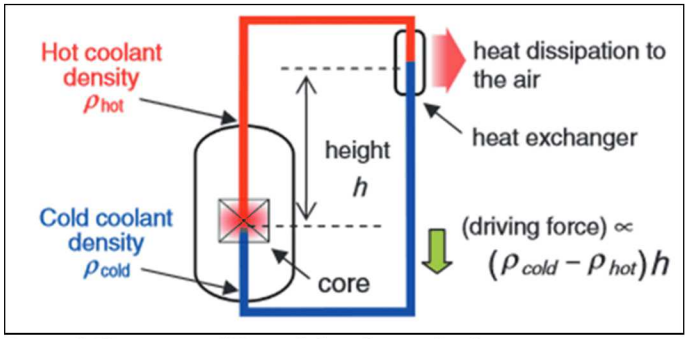

Figure 1 Illustration of Natural Circulation Configuration.

Table 1 Comparison of reduced Grashof number for CO_2 and water near the critical point for CO_2.

Parameter	Units	CO_2	Water
Bulk Temperature	K	300	300
Wall Temperature	K	310	310
Pressure	MPa	7.69	7.69
β	1/K	0.039	0.00037
ρ	kg/m^3	275.6	996.7
μ	Pa-s	2.21e-5	6.94e-4
υ = μ/ ρ	m^2/s	8.02e-8	6.96e-7
Gr/D^3	m^{-3}	5.9e14	7.5e10

2. sCO_2 NATURAL CIRCULATION LOOP

In 2012, Sandia National Laboratories began assessing the potential of sCO_2 as the working fluid in a dry-cooled, natural circulation loop. There were two major focus areas for this project, establishing the potential for natural circulation and potential for dry heat rejection.

The loop was operated in four different configurations. This paper describes two of the configurations. In one configuration, the CO_2 was heated via a water-to-CO_2 heat exchanger and cooled with an Xchanger CO_2-to-air heat exchanger. In the second configuration, the CO_2 was heated via an induction heater and cooled via a single-pass tube and shell (concentric tube) CO_2-to-water heat exchanger.

Experimental results determined that the loop could be controlled utilizing both dry heat rejection and sCO_2-to-water heat rejection. Consistent natural circulation of sCO_2 was achieved, with up to approximately 0.33 lbm/sec (0.15 kg/sec) mass flow rate observed. Start-up from both single phase and two-phase conditions was achieved in a controllable manner.

2.1 Water-Heated, Air-Cooled sCO_2 Loop

The first configuration utilized a Sentry spiral tube water-to-sCO_2 heat exchanger for heating and an Xchanger forced air-to-sCO_2 cooling fan for cooling. The hot leg (a vertical section of 1 inch outside diameter (OD) Swagelok tube) of the loop in this configuration is 200 inches (approximately 508 cm) from the top of the Sentry heat exchanger to the top of the loop. The sCO_2 then runs horizontally inside the tube for 55 inches (approximately 140 cm) before entering the Xchanger cooling unit. It exits the cooling unit 30 inches (approximately 76 cm) lower than it enters. It then travels another 42 inches (approximately 107 cm) horizontally before traveling downward 154 inches (approximately 391 cm). At this point, the tube runs horizontally 94 inches (approximately 239 cm) before traveling downward another 16 inches (approximately 41 cm) to enter the Sentry heat exchanger again. Figure 2 is a schematic of the water-heated, air-cooled configuration of the sCO_2 natural circulation loop.

In this configuration, a Keltech Acutemp 50 kW heater was used to heat water. The water was then passed through the shell side of the Sentry spiral heat exchanger. The sCO_2 was passed through the tube side of the Sentry heat exchanger and heated by the water. The sCO_2 was then cooled via the Xchanger CO_2-to-air heat exchanger. The loop utilized 1" OD Swagelok tubing with a 0.095" wall thickness. After the CO_2 passed through either of the heat exchangers, it passed through a Micromotion F Series Coriolis Flow and Density meter. There were also thermocouples before and after each heat exchanger to measure temperature and pressure of the CO_2. A MarwinValve 3000 Series adjustable valve was installed on the cold leg that could be used to increase flow restriction.

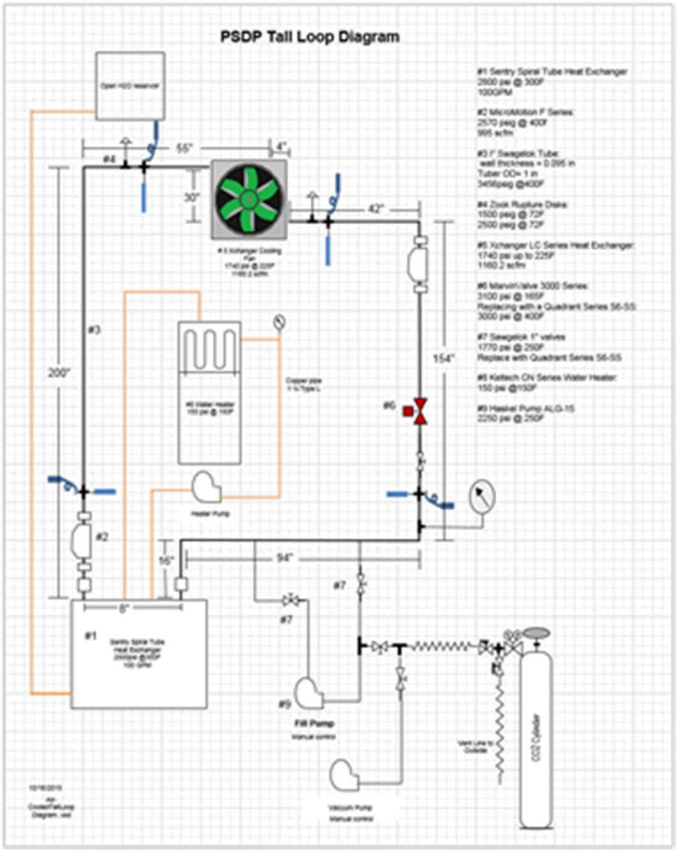

Figure 2 Schematic of water-heated, air-cooled sCO_2 natural circulation loop at Sandia National Laboratories.

2.2 Induction-Heated, Water-Cooled sCO_2 Loop

In the second configuration, the Sentry spiral tube heat exchanger was replaced by a Miller ProHeat 35 Liquid Cooled Induction Heating System along the length of the hot leg. The Xchanger cooling fan was also removed and replaced by a custom build tube-in-tube sCO_2-to-water heat exchanger.

Figure 3 is a conceptual design of the layout of the loop in this configuration. As can be seen from the figure, the wall temperature on the "hot leg" was measured at 6 locations using thermocouples. The "cold leg" wall temperature was measured in 5 locations with thermocouples. The CO_2 bulk temperature was also measured at 5 locations along the cold leg with resistance temperature detectors (RTDs). Figure 4 is a schematic of the loop in this configuration.

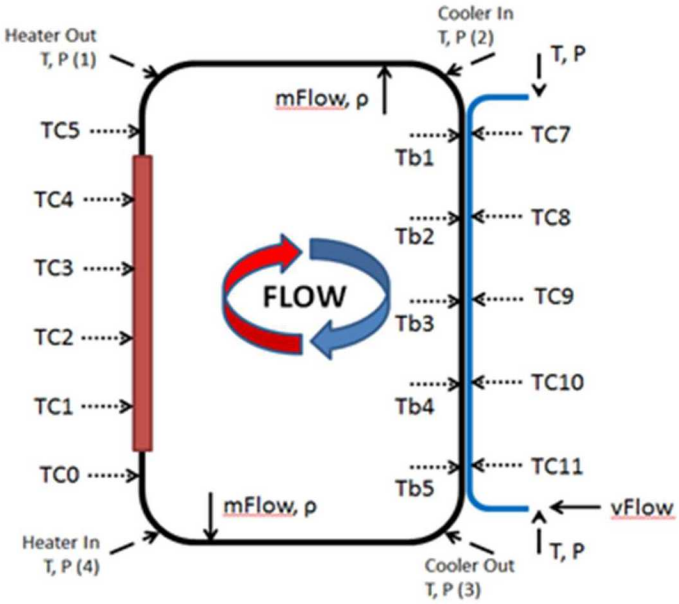

Figure 3 Conceptual layout of induction heated, water-cooled sCO_2 natural circulation loop at Sandia National Laboratories.

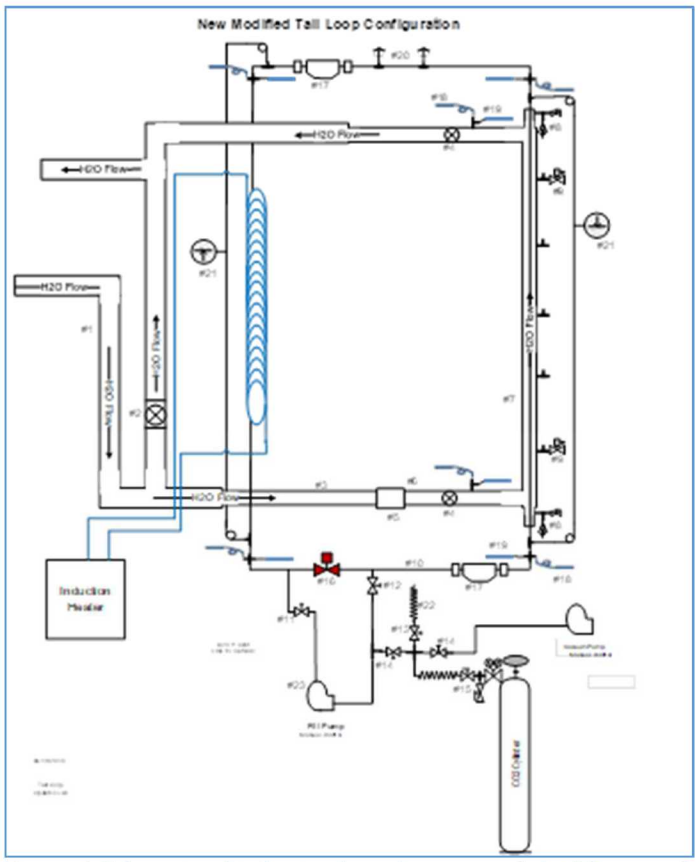

Figure 4 Schematic of induction heated, water-cooled sCO_2 natural circulation loop at Sandia National Laboratories.

3. EXPERIMENTAL RESULTS OF sCO_2 NATURAL CIRCULATION LOOP OPERATION

The sCO_2 natural circulation loop was operated for nine months under various configurations. This section describes some results for the two configurations introduced in Section 2.

3.1 Water-Heated, Air-Cooled Results

The first test was conducted to qualitatively determine how the system responded to changes in mass loading. To ensure initial flow in the desired direction, the cooler fan was turned on before the loop was heated. The aim was to create a cold slug of CO_2 at the top of the cold leg, thereby ensuring an initial driving force in desired flow direction.

After heating and establishing initial flow, mass was added to the loop in step increments. The modified Grashof number for a loop of uniform diameter in steady-state operation can be calculated according to equation (2) [12].

$$Gr_m = \frac{4DgQH}{\pi}\frac{\rho^2\beta}{c_p\mu^3} \tag{2}$$

The first fraction in this equation is a constant for a given heat rate (Q); the second fraction is variable. As mass is added to the loop, density obviously increases. However, the other three terms are not monotonic in their behavior with increasing pressure. Figure 5 shows a plot of this factor as a function of temperature at four different pressures. It is difficult to tell from this plot whether the modified Grashof number will increase or decrease with added mass.

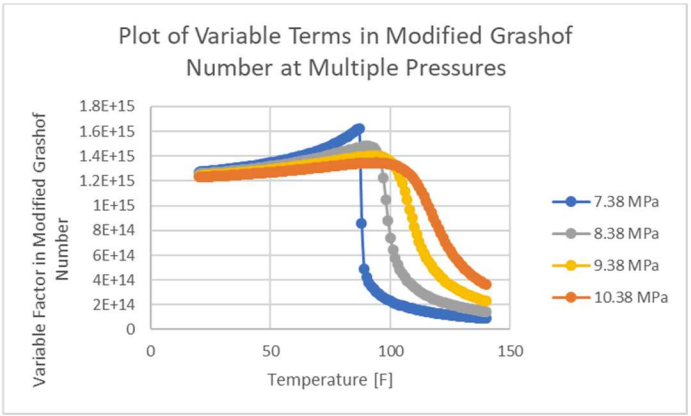

Figure 5 Plot of variable term in loop modified Grashof number versus temperature for four pressures above the critical pressure.

Neglecting the changes due to the heat exchangers, the Grashof number (for turbulent flow) is also related to the steady-state Reynolds number via equation (3) [10].

$$Re_{ss} \equiv \frac{\rho u D}{\mu} = \frac{\dot{m}D}{A_c\mu} = 1.9561\left(\frac{Gr_m}{L_t/_D}\right)^{0.36364} \tag{3}$$

From this equation, it is obvious that the mass flow rate is a monotonically increasing function of the modified Grashof number. This behavior was observed in the mass-loading experiment. Figure 6 displays the result of the experiment, which lasted about eight hours.

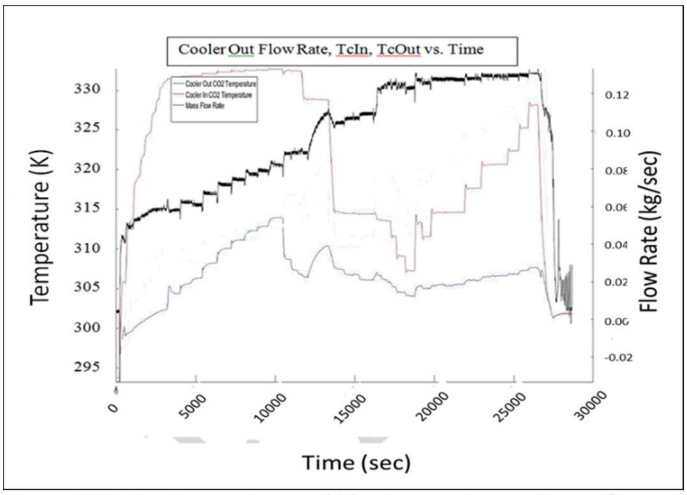

Figure 6 Hot leg temperature, cold leg temperature and mass flow rate of CO_2 resulting from the mass-loading experiment in a supercritical CO_2 natural circulation loop at Sandia National Laboratories.

As can be seen in Figure 6, the mass loading increments began about 60 minutes into the experiment. Each step increase in mass resulted in a step increase in mass flow rate, as well as a step increase in cold leg temperature. However, the hot leg temperature remained relatively constant. The increase in mass flow rate is due to the first law conservation of energy, as indicated in equation (4). As temperature increases, specific enthalpy increases, but the heat rate remained constant. From Figure 6, the cold leg temperature increased significantly more than the hot leg temperature. Therefore, the flow rate decreased.

$$\dot{m} = \frac{Q}{h_{hot} - h_{cold}} \tag{4}$$

About 10000 seconds into the experiment, the cooler fan power was increased. This caused a quick decrease in cold leg temperature and a corresponding increase in mass flow rate (from ~10000 seconds until ~12000 seconds in Figure 6). Step increases in fan power were continued until about 18000 seconds into the experiment.

At about 18000 seconds into the experiment, the CO_2 had cooled enough to test system response to increases in heat rate. At all times between the initial establishment of steady state flow (~3500 seconds into the experiment) and the shutdown initiation (~26000 seconds into the experiment), both the hot leg and the cold leg temperatures were above the critical temperature.

Thus, during this phase of the experiment, the density changes were not as great as would be possible near the critical point, or even in the compress fluid state. Figure 7 shows a temperature-density plot with the temperature differences observed during the heat rate variation experiment marked. The states marked in blue are approximately those observed at the beginning of the heat rate experiment (~19000-20000 seconds). Those marked in red are approximately the states observed after the last increase in heat rate (~26000-27000 seconds). As can be seen from this figure, a small increase in cold leg temperature (nearer the critical point) would need a much larger increase in hot leg temperature (further from the critical point) to obtain the same density difference. This behavior was observed in this portion of the experiment. The relatively constant density difference between the hot and cold portions of the CO_2 resulted in a nearly constant mass flow rate, even though the heat rate, as well as the hot leg temperature, increased.

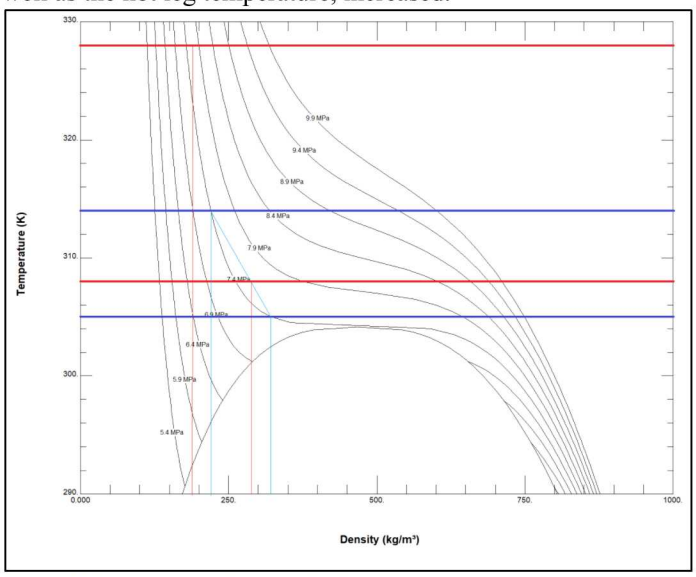

Figure 7 Temperature density plot for CO_2.

3.2 Induction-Heated, Water-Cooled Results

The goal of the experiment that was conducted using the induction-heated, water-cooled configuration was to monitor the response of the system under increases in heat rate. Although the induction heater is rated at 50 kW, the limits on the Sandia loop were limited to between 10 and 15 kW. This was due to the use of austenitic stainless steel tubing, which has a lower magnetic permeability than the metal used to calibrate the heater. Figure 8 shows a power cascade of the experiment. As can be seen, the heater actual power was less than the commanded power. This discrepancy became more apparent at higher power levels. It also resulted in lower heat rates. However, the heat rates were adequate for the testing.

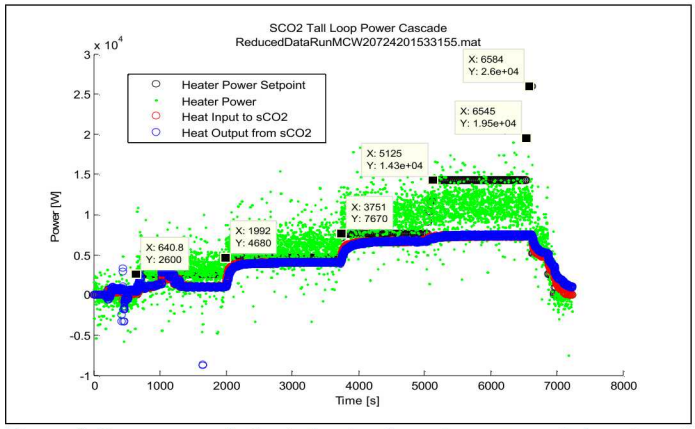

Figure 8 Power cascade for induction-heated, water-cooled testing of Sandia natural circulation sCO_2 loop.

Initial startup took about 1300 seconds, at which time heat rate was held constant at 2.6 kW for about 700 seconds. Increases in power to 4.0 kW, 6.5 kW, and 7.3 kW were implemented over the course of the experiment. Figure 9 shows mass flow rate, temperatures, pressures, and heat rate for the experiment.

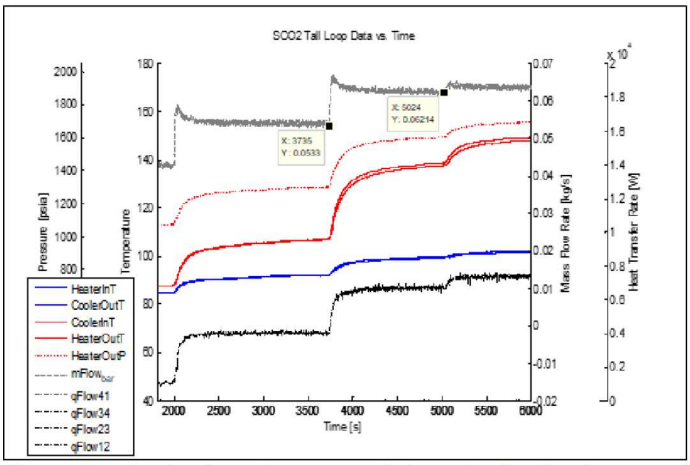

Figure 9 Induction-heated, water-cooled results for Sandia natural circulation sCO_2 loop.

The mass flow rates responded as expected overall. However, there are some overshoots in the flow rates at the beginning of each power increase. Since flow rate is driven by differences in density of the hot and cold legs, which are in turn driven by differences in temperature, the initial thought was that the bulk temperature of the water should mirror this flow rate response. That was not the case. This is a transient response and could have to do with the fast response of the hot side wall temperature due to induction heating.

3.3 Results Summary

The results of the experiments tested at the Sandia National Laboratories sCO_2 natural circulation loop verify that such a loop can be operated in a controlled manner. These results – especially those related to the water-heated, air-cooled configuration – indicate that with the correct design and control scheme, such a loop could possibly be used to retrofit existing water-cooled power plants and convert their cooling system to a hybrid cooling system. This has been the subject of Sandia's Waterless Power program since Fall 2015.

4. DISCUSSION

The purpose of the experimental work reported in Middleton, et al [7] and outlined in Sections 2 and 3 of this technical paper was based on the possibility of developing a sCO_2 decay heat rejection system (DHS) for small modular nuclear reactors (SMRs). However, there is no difference in this application and that of transferring heat from a power plant's cooling water to ambient air. To this end, Sandia began investigating ways to develop an indirect dry cooling technology that can be coupled with existing power plant cooling systems to cost-effectively reduce water use at the plants.

One of the major drawbacks to dry cooling is the large efficiency penalty incurred by the power plant due to having to reject heat at the dry bulb temperature instead of the wet bulb temperature. Coupled with the high cost of fans needed to drive air over the heat exchangers and pumping power required to re-route the plant coolant, this can be the major driver in rejecting dry cooling options. Recent advances by Johnson Controls, Inc. (JCI) have mitigated some of these deficiencies in dry cooling [11, 12].

The JCI BlueStream Thermosyphon (TSC) utilizes r134a as a working fluid to reject heat to ambient air. The design allows for re-routing the plant coolant with little to no pumping power. The working fluid of the TSC is heated by the water, evaporates in the evaporator, and rises to the condenser, where it is condensed by forced air.

Sandia researchers submitted a technical advance (TA) in 2015 to improve on the operation of a device such as the TSC. In 2017, a patent application was submitted by Sandia and the patent was awarded on January 22, 2019 [10].

The basis for the patent application is the use of either a supercritical fluid or a zeotropic fluid. Both fluids increase in temperature when heat is rejected into them. Supercritical fluids do this because they never become two-phase; zeotropic fluids do this via a temperature glide in the two-phase regime. There are three benefits to a power plant related to this temperature change.

The first benefit is that the minimum temperature to which the water can be cooled is lower than that of a single two-phase refrigerant with the same average operating temperature. Figure 10 shows a hypothetical cooling situation for a thermosyphon with a single two-phase refrigerant operating at 30˚ C. For an approach of 5˚ C in the water-to-refrigerant heat exchanger, the minimum temperature of the water is 35˚ C. On the other hand, for the same ambient conditions and same water inlet temperature, a supercritical fluid operating at an average temperature of 30˚ C could cool the water to a lower temperature. Figure 11 illustrates this scenario.

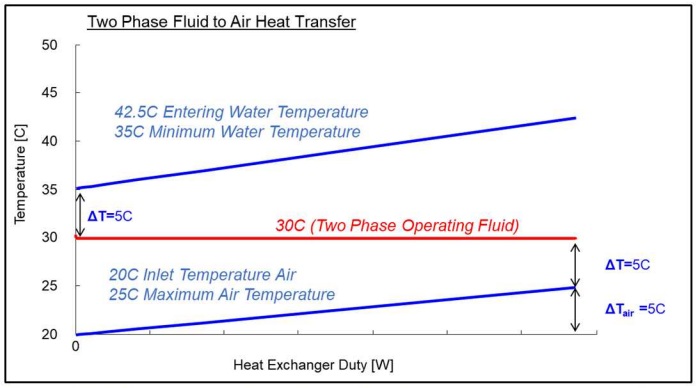

Figure 10 Schematic for hypothetical cooling scenario using single two-phase operating fluid in a thermosyphon.

In the scenario presented, the minimum working fluid temperature is 25˚ C and the maximum working fluid temperature is 35˚ C, for an average temperature of 30˚ C. The

water inlet temperature and the ambient air temperature are the same as that for the thermosyphon operating with a single two-phase refrigerant. The assumed approach temperature for the water-to-refrigerant heat exchanger is also the same. However, the water can be cooled to 30˚ C (instead of 35˚ C). The lower cooling limit can result in much more dry heat rejection. Assuming a nearly constant specific heat capacity for water and all other conditions being equal between the two scenarios, the supercritical thermosyphon would reject about 67% more heat than the two-phase thermosyphon. Equations (5) and (6) are used to demonstrate this result.

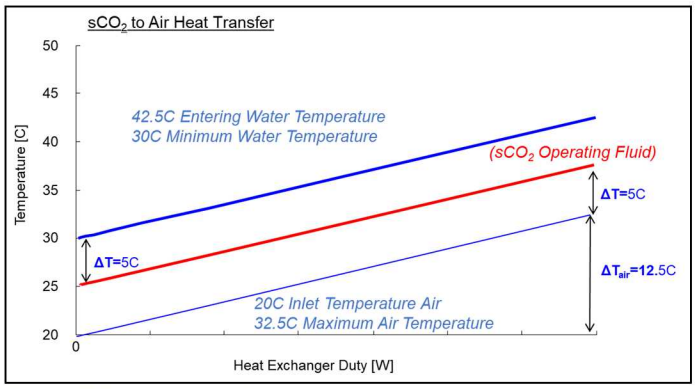

Figure 11 Schematic for hypothetical cooling scenario using supercritical fluid or zeotropic fluid in a thermosyphon.

$$Q_{H2O} = \dot{m}_{H2O} c_p (T_{exit} - T_{in}) \quad (5)$$

Since the mass flow rate and specific heat capacity are assumed to be constant, we have the following ratio.

$$\frac{Q_{H2O}^{SC}}{Q_{H2O}^{2p}} = \frac{30-42.5}{35-42.5} = {}^{5}/_{3} \quad (6)$$

The second benefit of using a supercritical fluid or zeotropic fluid is that the air being used as the ultimate heat sink can be raised to a higher temperature for the same average operating fluid temperature. This can again be seen by comparing the scenarios in Figures 10 and 11. In both cases, the air enters at 20˚ C. In the case of a single two-phase operating fluid at 30˚ C with a 5˚ C approach, the maximum air temperature is only 25˚ C, whereas it is 32.5˚ C in the supercritical thermosyphon.

Assuming a constant heat capacity for air – which is a conservative estimate as the heat capacity for air increases with temperature – each unit mass of air would be capable of absorbing 2.5 times as much heat as in the two-phase operating fluid case, which is easily seen with a first law analysis (applying equation 4 to air). In other words, although the supercritical thermosyphon can reject 5/3 of the heat rejected by the two-phase thermosyphon, it requires only 2/3 of the air flowrate. This can be determined by dividing the ratio of heat rejected by the ratio of total heat capacity of the air, as demonstrated in Equation (7).

$$F = \frac{{}^{5}/_{3}}{{}^{5}/_{2}} = {}^{2}/_{3} \quad (7)$$

The reduction is air flow needed to reject heat is the third benefit of the SNLNCC. Air flow is normally affected by using electricity to power large fans. Two nominal fan laws are shown in Equations (8) and (9).

$$\dot{V}_2 = \dot{V}_1 \times \frac{RPM_2}{RPM_1} \quad (8)$$

$$P_2 = P_1 \times \left(\frac{RPM_2}{RPM_1}\right)^3 \quad (9)$$

Equation (8) says that volumetric flow rate is proportional to the rotational speed of the fan. Equation (9) says that the power required to drive a fan is proportional to the cube of the rotational speed of the fan. Therefore, the power required to drive a fan is proportional to the cube of the volumetric flow rate of air. In the scenario presented above, the fan power required for the SNLNCC should be about equal to F^3, where F is defined in Equation (7).

$$\frac{P^{SC}}{P^{2p}} = F^3 = \left({}^{2}/_{3}\right)^3 = {}^{8}/_{27} \approx 30\% \quad (10)$$

This means that a supercritical thermosyphon operating at the same average temperature as a two-phase thermosyphon under the conditions hypothesized in Figures 10 and 11 should be able to reject about 1.67 times as much heat as the two-phase thermosyphon while requiring only 30% of the fan power.

CONCLUSIONS AND FURTHER WORK

The work conducted at Sandia from 2012 through 2015 demonstrated that natural circulation of supercritical CO_2 can improve dry heat rejection. This work was leveraged to develop a patent on supercritical and zeotropic thermosyphons. Currently, Sandia is working with industry and with the Department of Energy to advance the technology with plans to deploy in the next few years.

REFERENCES

[1] Bauer, Diana, "Water-Energy Nexus: Challenges and Opportunities," US Department of Energy, Office of Energy Policy and Systems Analysis, Water-Energy Tech Team (WETT), September 5, 2014.

[2] Wang, Jiao, Lean Schleiter, Lijin Zhong (2019, June 29). *No Water, No Power*. Retrieved from https://www.wri.org/blog/2017/06/no-water-no-power.

[3] Flessner, Dave (2010, August 23). *Browns Ferry Plant in Hot Water*. Retrieved from http://archive.knoxnews.com/business/browns-ferry-plant-in-hot-water-ep-407834721-358564491.html/.

[4] Union of Concerned Scientists (2013, July 15). *How it Works: Water for Power Plant Cooling.* Retrieved from https://www.ucsusa.org/resources/water-power-plant-cooling.

[5] U.S. Congressional Research Service. Cooling Water Intake Structures: Summary of the EPA Rule (September 8, 2014).

[6] Ray, Suparna (2018, August 29). *Some U.S. electricity generating plants use dry cooling.* Retrieved from https://www.eia.gov/todayinenergy/detail.php?id=36773#.

[7] Middleton, Bobby D., Salvador Rodriguez, and Matthew Carlson (2015) Design, Construction, and Operation of a Supercritical Carbon Dioxide Loop for Investigation of Dry Cooling and Natural Circulation Potential for Use in Advanced Small Modular Reactors Utilizing sCO_2 Power Conversion Cycles. SAND2015-10092. Albuquerque, NM.

[8] Middleton, Bobby, Matthew D. Carlson, and Marie Y. Arrieta (2019). *United States Patent No. US 10184726 B1.* Retrieved from http://patft.uspto.gov/netacgi/nph-Parser?Sect1=PTO1&Sect2=HITOFF&d=PALL&p=1&u=%2Fnetahtml%2FPTO%2Fsrchnum.htm&r=1&f=G&l=50&s1=10184726.PN.&OS=PN/10184726&RS=PN/10184726.

[9] Conboy, Thomas, "S-CO_2 as an Enabling Technology for Dry-Cooled Nuclear Power," Presented at ASME 2014 Small Modular Reactors Symposium, Washington, DC, April 15, 2014.

[10] Vijayan, P.K., M.R. Gartia, D.S. Pilkhwal, A.K. Hayak, and D. Saha, "Steady State Flow in Single-Phase and Two-Phase Natural Circulation Loops," 3rd IASME/WSEAS International Conference on Heat Transfer, Thermal Engineering, and Environment, August 20-22, Corfu Island, Greece.

[11] Carter, Thomas P., Sean P. Bushart, James W. Furlong, and Jessica Shi (2014) 'Wet, Dry, and Hybrid Heat Rejection System Impacts on the Economic Performance of a Thermoelectric Power Plant Subjected to Varying Degrees of Water Constraint', *ASME 2014 Power Conference*, Baltimore, MD, 28-31 July, POWER2014-32051.

[12] Sickinger, David, Otto Van Geet, Suzanne Belmont, Thomas Carter, and David Martinez (2018) Thermosyphon Cooler Hybrid System for Water Savings in an Energy-Efficient HPC Data Center. NREL/TP-2C00-72196. NREL, Boulder, CO.